

Constrained Reinforcement Learning for Safe Heat Pump Control

Baohe Zhang^{*†}, Lilli Frison^{*§}, Thomas Brox[†], Joschka Bödecker[†]

Abstract—Constrained Reinforcement Learning (RL) has emerged as a significant research area within RL, where integrating constraints with rewards is crucial for enhancing safety and performance across diverse control tasks. In the context of heating systems in the buildings, optimizing the energy efficiency while maintaining the residents’ thermal comfort can be intuitively formulated as a constrained optimization problem. However, to solve it with RL may require large amount of data. Therefore, an accurate and versatile simulator is favored. In this paper, we propose a novel building simulator I4B which provides interfaces for different usages and apply a model-free constrained RL algorithm named constrained Soft Actor-Critic with Linear Smoothed Log Barrier function (CSAC-LB) to the heating optimization problem. Benchmarking against baseline algorithms demonstrates CSAC-LB’s efficiency in data exploration, constraint satisfaction and performance.

I. INTRODUCTION

Europe’s energy landscape is with approximately 40% of its energy consumption allocated to heating, predominantly fueled by non-renewable sources. The urgency to transition towards more sustainable energy practices is palpable, as numerous European nations set ambitious targets to slash emissions in the heating sector by 40% by 2030 compared to 1990. This imperative move is not just a step towards meeting climate objectives but also a significant leap towards redefining energy efficiency within the heating domain.

Enhancing the efficiency of heating systems emerges as a cornerstone in this endeavor, necessitating the wide applications of innovative technologies in electricity and heating networks. Such integration, particularly at the building or district level, is pivotal for substantially reducing energy consumption. Heating systems, whether in residential buildings or commercial establishments, are critical for maintaining comfort and energy efficiency. Applying constrained reinforcement learning (RL) algorithms to solve heating system control problems presents a compelling approach due to several advantages. Constrained RL methods are not only capable to address the balance between thermal comfort and energy usage, but also learn in real-time data from noisy sensor observations as proven in many robotic tasks [1]. It also allows the agent to continuous learning in dynamical scenario when building uses or electricity price evolve.

The role of simulation frameworks in training RL agents is undeniably crucial. The success of Issac Gym [2] has significantly accelerated the development in many robotics tasks (e.g. locomotion [3]). An accurate, adaptable, and parallelizable simulator can substantially accelerate the policy

improvement cycle, enabling more precise control over heating systems.

Despite there are many frameworks coming up within the realm of heating control, a comprehensive open-source lightweight simulation framework which provides a handful of simulated building environments, extensive customization options and serves as a conduit between the control community and Reinforcement Learning community through a standardized interface is still missing. To bridge this gap, we propose a novel open-source framework Intelligence for Building (I4B) for simulation-based advanced control strategies such as model predictive control (MPC) and RL, for heat pump operation. I4B creates an interface between the building simulation module and the control algorithm, incorporating reference controllers, support for parallelization, and standardized metrics for evaluating algorithms.

We conceptualize the heating control problem as a constrained Markov Decision Process (CMDP), where the objective is to minimize energy usage while maintaining indoor temperature above a predefined threshold. Upon applying state-of-the-art constrained RL algorithms to this framework, our empirical investigation benchmarks their performance across various scenarios. Noteworthy among these algorithms is the constrained RL with linear smoothed log barrier function (CSAC-LB), a novel approach which particularly suits the heating control problem. Heating system problem is characterized by an optimal solution that lies at the boundary of the feasible and infeasible sets. Our findings reveal that CSAC-LB excels in balancing exploration with performance. To summarize, our contributions are following:

- We propose I4B¹, a novel open-source lightweight building heat pump operation simulator with rich customization options and interfaces for different research communities.
- We applies variety of constrained RL algorithms to different heating scenarios. An empirical study is performed to benchmark them.
- We demonstrate CSAC-LB can balance the objective and constraints better compared to other SOTA methods.
- We perform a comprehensive analysis on it compared to other algorithms in the context of heating control problem.

II. RELATED WORK

A. RL in building heating control

In recent years, reinforcement learning (RL) has gained attraction as a method for optimizing the operation of building

*: These authors contributed equally

†: Faculty of Computer Science, University of Freiburg, Germany. §: Fraunhofer Institute for Solar Energy Systems, Germany. Contact Address: zhangb@cs.uni-freiburg.de

¹Publicly available under <https://github.com/lfrison/i4b>.

heating, ventilation, and air conditioning (HVAC) systems. A good overview is provided in the recent article [4]. Different RL variants, called static and dynamic, are proposed in [5]. Their findings also indicate that a heating energy saving ranging between 5 and 12% is possible compared to standard heating curve control. A significant amount of current works focus on the comparison of model-free RL with various control strategies such as MPC, model-based RL, data-driven control methods, and other hybrid approaches [6]. The subject to many papers is the comparison of Model-free RL to ideal MPC, such as in [7]. Many contributions, such as or [6], additionally consider model-based RL or data-driven control as hybrid approach between MPC and model-free RL. The publication [8], for instance, compares MPC and RL. The algorithms are implemented and evaluated in BOPTTEST, a standardized simulation framework for the assessment of advanced control algorithms in buildings. The results indicate that pure RL cannot provide constraint satisfaction. Therefore, a hybrid algorithm called reinforced predictive control (RL-MPC) that merges their relative merits, is proposed. Another approach is learning-based MPC, as discussed in [9], where a deep neural network is employed to learn the model, which is subsequently used for optimization. In summary, despite progress in applying RL to building heating control, a detailed examination of advanced RL algorithms, especially those tackling state constraints through constrained RL, requires further investigation.

B. Constrained RL algorithm

Many comprehensive reviews of Constrained Reinforcement Learning [10], [11] have been published in the recent years. One notable approach in addressing constrained RL problems is safe policy search methods. These methods often incorporate nonlinear programming techniques into policy gradient frameworks or develop safe policy search strategies based on theoretical analyses [12], such as gradient projection [13], [14]. Extensions [15] to safe policy search include the integration of Gaussian Process models for risk estimation. Constrained Policy Optimization (CPO) [16] method and its successor [17] serve as general-purpose approaches, utilizing trust-region methods to solve constrained RL problems while offering theoretical guarantees. Additionally, Conditional Value-at-risk (CVaR) [18], [19] has been used to optimize Lagrangian functions with gradient descent, further enriching this research area. In [20], [21], the authors extend SAC [22] with a cost function and optimize the constrained problem by introducing a Lagrange-multiplier. Further improvements are presented in [23] where a distributional safety critic is combined it with the CVaR metric. Applying interior-point methods to on-policy RL algorithms [24], [25] are also drawing many attentions in the recent development. Another line of work is close to MPC. Model-based approaches, such as in [26], utilize dynamics models to certify safety but are often limited by assumptions about model accuracy and known constraints.

C. Building Simulator

Over the past decades, several frameworks for simulating the thermal building behavior for application to control strategy development and testing have been developed. Energym [27] is an open source building simulation library designed to test climate control and energy management strategies on buildings in a systematic and reproducible way. It relies on the functional mockup interface (FMI) standard in order to support models developed in the modelling languages Modelica and EnergyPlus. Bobtest (Building Operation TESTing) [28] is a newer framework consisting of a set of Modelica models that represent different buildings with different HVAC systems in different climate zones. Sinergym [29] was developed particularly to create an environment following Gymnasium [30] interface for wrapping the building simulation engines EnergyPlus for building control using deep reinforcement learning. Most environments require the user to either manually install a building simulator (e.g. EnergyPlus) or to manually manage Docker containers. This can be tedious. For this reason, Beobench [31] was introduced as a toolkit providing easy and unified access to different building control environments for RL. Unfortunately, due to the complexity of creating building simulations, none of the existing frameworks provides more than a handful of simulated buildings.

III. CONSTRAINED RL

A. Constrained Markov Decision Processes

A Constrained Markov Decision Process (CMDP) is an extension of a Markov Decision Process (MDP), defined by the tuple (S, A, R, γ, P) , where S represents the set of states, A denotes the set of actions, $R : S \times A \rightarrow \mathbb{R}$ is the reward function, γ is the discount factor, and P is the probabilistic state transition model.

To construct a CMDP, we augment the MDP with a cost function $C : S \times A \rightarrow \mathbb{R}^K$, which incorporates a set of constraints and yields a K -dimensional vector of costs for each state-action pair. Here, $J_C(\pi)$ represents the expected cumulative discounted cost under a given policy π , and D is a K -dimensional vector of cost limits.

The feasible set of policies for a CMDP, denoted as Π_C , is defined as follows:

$$\Pi_C = \{\pi \in \Pi : J_C(\pi) - D \leq 0\} \quad (1)$$

Where Π represents the set of all possible policies. In this context, $J(\pi)$ represents the expected cumulative return to be maximized. Therefore, the optimization problem of learning an optimal policy can be formulated as:

$$\pi^* = \arg \max_{\pi \in \Pi_C} J(\pi) \quad (2)$$

This optimization seeks the policy π^* that maximizes the return while adhering to all constraints defined by the cost function C .

B. Linear Smoothed Log Barrier Function

The log barrier method is recognized for its capability to address constrained optimization problems that include inequality constraints, yet it is prone to challenges with numerical stability. This instability arises because the logarithmic function within the log barrier method cannot accommodate conditions where $g(x) > 0$, leading to difficulties in maintaining stable optimization.

In the realm of Deep RL, where neural networks are employed to approximate value functions and model continuous control policies, the issue of constraint satisfaction becomes particularly pronounced. Due to the inherent randomness in initializing neural network parameters, the policy defined by the actor network might initially violate some constraints, thus outlining an unsafe policy. A straightforward workaround might involve clipping the network's output values to the output layer to mitigate constraint violations. However, these approaches may stop gradient flow during the optimization process or even overlook constraint violations entirely.

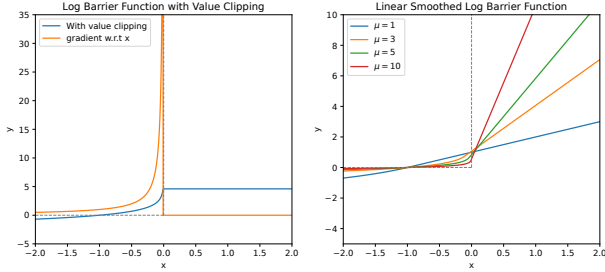


Fig. 1: **Left:** Log barrier function (Blue curve) with Value Clipping. Due to the value clipping when $y = 5$, the gradient vanishes. **Right:** Linear smoothed Log barrier function with different μ . The dashed line is the indicator function.

To solve these drawbacks associated with directly clipping the neural network's output, a novel approach involving a linear smoothed log barrier function [32], $\tilde{\psi}(x)$, has been introduced. This function is designed as follows:

$$\tilde{\psi}(x) = \begin{cases} -\frac{1}{\mu} \log(-x) & \text{if } x \leq -\frac{1}{\mu^2} \\ \mu x - \frac{1}{\mu} \log(\frac{1}{\mu^2}) + \frac{1}{\mu} & \text{otherwise} \end{cases} \quad (3)$$

where μ is a parameter that adjusts the function's behavior. The key advantage of $\tilde{\psi}(x)$ lies in its continuous and differentiable nature across its entire domain, allowing for the application of stochastic gradient descent (SGD) without being confined solely to the feasible set. This facilitates a more robust and flexible approach to optimizing neural networks in the context of constrained RL.

C. SAC-Lag

Originally developed for teaching quadruped robots locomotion [20], SAC-Lag adapts the Soft Actor-Critic framework [22] by incorporating stepwise constraints to limit the robot's pose, aiming to mitigate potential damage. To define this constrained optimization task, we introduce d_t as the permissible threshold for constraint violations at each step

t , with the primary goal being to maximize the following objective:

$$\begin{aligned} & \sum_{t=0}^T \mathbb{E}_{a_t \sim \pi(s_t)} \left[\gamma^t R(s_t, a_t) + \alpha H(\pi(\cdot|s_t)) \right] \\ \text{s.t.} & \mathbb{E}_{a_t \sim \pi(s_t)} \left[C(a_t, s_t) - d_t \right] \leq 0, \forall t \end{aligned} \quad (4)$$

where R is the reward function and $H(\pi(\cdot|s_t))$ is the entropy term. As in [21] using the Lagrange-multiplier method, we denote d as the cumulative cost limit. The unconstrained optimization problem can be formulated as:

$$\max_{\pi} \min_{\beta \geq 0} L(\pi, \beta) \doteq f(\pi) - \beta g(\pi) \quad (5)$$

$$\begin{aligned} \text{where } f(\pi) &= \sum_{t=0}^T \mathbb{E}_{a_t \sim \pi(s_t)} \left[\gamma^t R(s_t, a_t) + \alpha H(\pi(\cdot|s_t)) \right] \\ \text{and } g(\pi) &= \sum_{t=0}^T \mathbb{E}_{a_t \sim \pi(s_t)} \left[\gamma^t (C(a_t, s_t) - d) \right] \end{aligned}$$

Given that the Q-value is approximated using neural networks, Equation 5 lacks a closed-form solution. Consequently, Dual Gradient Descent [33] is employed to iteratively refine both the policy, parameterized by ϕ , and the Lagrange multiplier. The actor network's parameters are denoted by ϕ , and D represents the replay buffer. We denote the reward Q-network with parameters θ_r as Q_{θ_r} and the cost Q-network with parameters θ_c as Q_{θ_c} . To minimize Eq. 5, Lagrange-multiplier β is updated according to the following loss:

$$J(\beta) = \mathbb{E}_{s_t \sim D, a_t \sim \pi_{\phi}(s_t)} \left[\beta (d - Q_{\theta_c}(s_t, a_t)) \right] \quad (6)$$

This adjustment mechanism increases β when the cost Q-network's output surpasses the limit d , thereby tightening the constraints, and decreases it as the current policy becomes more likely to satisfy these constraints.

Now, assuming a fixed value for β , the actor loss to be minimized from Eq. 5 can be written as:

$$J(\phi) = \mathbb{E}_{s_t \sim D, a_t \sim \pi_{\phi}(s_t)} \left[\alpha \log \pi_{\phi}(a_t|s_t) - Q_{\theta_r}(s_t, a_t) + \beta Q_{\theta_c}(s_t, a_t) \right] \quad (7)$$

D. CSAC-LB

With the help of the linear smoothed log barrier function, we are able to solve the constrained RL problem via SGD. CSAC-LB [34] follows the setup of SAC-Lag [21] and uses double-Q critic networks not only to learn the reward but also the cost of constraint violation by taking the maximum of the two cost critic networks. This approach helps mitigate the underestimation of the Q-value of cost caused by constraint violations. This is especially helpful for heating systems in the collected replay buffer, where most of the transitions are free of constraints, subsequently causing an underestimation of the Q-value for cost.

The linear smoothed log barrier function maintains a minimal, non-zero gradient even when constraints are met, resulting in a sub-optimal solution. To address this and ensure convergence towards the optimal solution of the original RL objective while adhering to constraints, CSAC-LB introduces a modification by applying a ReLU activation to the input of $\psi(x)$, shifting it +1 along the positive axis. This adjusted variant is referred to as $\tilde{\psi}^*(x)$, with d representing the cost limit, x being the estimation of the Q-value from the cost critic network, and $\mu > 1$:

$$\tilde{\psi}^*(x) = \psi(\text{ReLU}(x - d) - 1) \quad (8)$$

Applying CSAC-LB to heating system control offers a distinct advantage: given the specific nature of the objectives and constraints in these tasks, the optimal solution typically resides at the boundary between the feasible and infeasible sets. This positioning encourages exploration along the boundary, enhancing the agent's accuracy in estimating Q-values for both rewards and costs. Leveraging the linear smoothed log barrier function, CSAC-LB facilitates more focused exploration within valuable areas, significantly boosting data efficiency. In contrast, methods based on Lagrangian updates may engage in excessive, less productive exploration within either the feasible or infeasible sets due to their inherent update mechanisms and the data distribution in the replay buffer.

IV. CONTROL TESTING FRAMEWORK FOR BUILDING HEAT PUMP OPERATION

A. Definition

A thermal building energy model is a mathematical description of the thermal energy-related behavior of a building, including details about its structure, systems, usage, and location. Various factors are considered, such as:

- Building envelope: This includes characteristics such as size, shape, layout, and orientation, as well as the construction and insulation.
- HVAC Systems: The heating, ventilation, and air conditioning systems are modeled, including their energy sources, efficiency, control strategies, and distribution methods.
- Internal loads: These represent the energy consumed within the building, including lighting, appliances, and equipment, as well as the heat produced by the occupants.
- Weather

They are used to simulate and analyze the energy performance of buildings, enabling predictions about energy consumption, cost, efficiency, and environmental impact, as well as, developing and testing different advanced control strategies. There are different control tasks that arise in building heating operation, such as:

- Reference tracking: Keep room temperature close to the set point temperature despite disturbances such as heat loss to the ambient and heat gains due to people behavior and solar irradiations.

- Additionally minimize an "economic" cost function (e.g., energy cost).
- Demand responsive heating and cooling operation for improving the stability of the electric grid.

B. Requirements and software architecture

The requirements for a heat pump control testing framework can be specified as follows:

- Emulation models including HP, building, and heating emission to simulate the physics, dynamics, and time-resolution necessary for controls design
- Standardized simulation environment for consistent benchmarking results
- Well defined data exchange interface between a test controller, the emulator models and the simulation engine
- Provide exogenous input data (weather, user profiles, energy prices, ...)
- Standardized KPIs for evaluation
- Open source software, good documentation
- Easy to use, fast solution time and easy debugging for external users
- Easy adaptation to the specific heat pump system (heat emission system, DHW, PV integration, large-scale heat pump. ...)

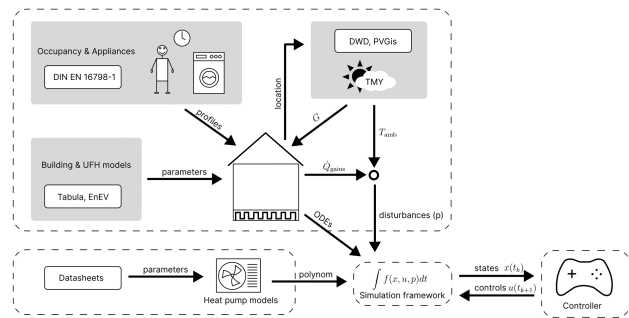


Fig. 2: Overview of software architecture

The simulator architecture is illustrated in Figure 2. A simulator class provides a high level interface to perform one and multi-step simulations that return the next state(s) of the building (temperatures) and indicators for comfort levels and the energy demand. This interface can be used to evaluate and test different control strategies. Simple heat pump models, based on performance curves, can be used as heating systems. Disturbance profiles for the ambient temperature, internal heat gains by occupancy, and appliances, as well as solar heat gains, can be generated. The goal of the simulation framework is to quickly generate a reduced-order model of a specific building and simulate this building. Additionally, the framework should be used for integration in control strategies. An overview of control method integration is shown in Figure 3. A simple rule-based heating curve controller can be used as the reference case at the lower performance base line. A MPC controller provides a reference case at the upper end. Furthermore, we also support Safety-Gymnasium-style [35] API for the RL community and it also supports vectorized environment for

parallel training. To maximize compatibility, a corresponding wrapper for Gymnasium-style and OpenAI Gym-style [36] API is also provided.

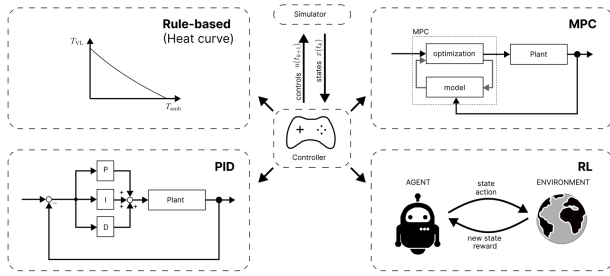


Fig. 3: Integration of controller

C. Thermal building models

Every model simplifies reality, often omitting certain phenomena, a principle particularly relevant to thermal behavior modeling in buildings, which involves complex interactions among internal conditions, external influences, and building materials.

We adopt a single-zone model for simulating building thermal dynamics, striking a balance between detail and computational efficiency. This model focuses on a water-based heating system, where heat, transferred from water through radiators or underfloor heating, circulates back to the heat source at a reduced temperature. This return temperature, considered a state in our model, along with the net energy flow, dictates the indoor temperature changes. While a more complex model might include additional temperature nodes for walls and differentiate between transmission losses and thermal mass, our three-state model simplifies this to indoor and wall temperatures, and water return temperature, as depicted in Fig. 4.

Exemplary, we describe the formulas for a two-state model with the state vector $x(t) = [T_{\text{room}}, T_{\text{hp,ret}}]$, capturing the thermodynamic interactions:

$$\dot{T}_{\text{room}} = 1/C_{\text{bldg}} \cdot (\dot{Q}_{\text{gain}} + H_{\text{rad,con}} \cdot (T_{\text{hp,ret}} - T_{\text{room}}) - H_{\text{ve,tr}} \cdot (T_{\text{room}} - T_{\text{amb}})) \quad (9)$$

$$\dot{T}_{\text{hp,ret}} = 1/C_{\text{water}} \cdot (\dot{m}_{\text{hp}} \cdot c_{\text{p,water}} \cdot (T_{\text{hp,sup}} - T_{\text{hp,ret}}) - H_{\text{rad,con}} \cdot (T_{\text{hp,ret}} - T_{\text{room}})) \quad (10)$$

Table I provides a definition of various building attributes and model quantities.

D. Heat Pump

From the heat pump supply and return temperatures, $T_{\text{hp,sup}}$ and $T_{\text{hp,ret}}$, and the usually constant mass flow in the building heat emission system \dot{m}_{hp} , the thermal heat pump power \dot{Q}_{hp} can be computed. To compute the heat pump efficiency, the following considerations are taken into account. A heat pump uses mechanical energy to transport heat energy from a lower to a higher temperature level. This process can be idealized

Symbol & Unit	Description
Input parameters $H_{\text{ve,tr}}$ [W/K] c_{bldg} [J/(m ² K)] A_{floor} [m ²] h_{room} [m]	Heat transfer coeff. of transmission & ventilation Specific heat capacity of building Conditioned floor area Average room height
Calculated parameters C_{bldg} [J/K] C_{water} [J/K] $H_{\text{rad,con}}$ [W/K]	Heat capacity of building envelope & thermal zone Heat capacity of water in HVAC system Heat transfer coeff. of the heating system
Time-var. parameters T_{amb} [°C] Q_{gains} [W]	Ambient temperature Internal and solar heat gains
States T_{room} [°C] $T_{\text{hp,ret}}$ [°C]	Temperature of the building Heat pump return flow temperature
Control $T_{\text{hp,sup}}$ [°C]	Heat pump supply temperature

TABLE I: Building model parameters

by a Carnot process. For the reversible Carnot process a theoretical COP of

$$\text{COP}_{\text{th}} = \frac{\dot{Q}_{\text{th}}}{P_{\text{el}}} = \frac{T_{\text{hp,sup}}}{T_{\text{hp,sup}} - T_{\text{amb}}} \quad (11)$$

is possible. However, real heat pumps do not operate loss-free. The achievable COP of a heat pump is therefore smaller than the theoretical value by the exergetic efficiency η_{WP} : $\text{COP} = \eta_{\text{WP}} \text{COP}_{\text{th}}$. Modern air-to-water heat pumps achieve an efficiency of about 0.45. Often the dependence of the COP on the source and sink temperature ($T_{\text{hp,sup}}$, resp. T_{amb} in Equation (11)) is approximated by a second-order polynomial that is fitted to manufacturer data.

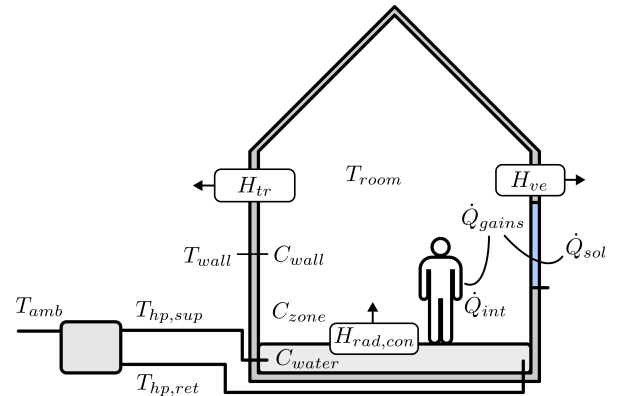


Fig. 4: Example thermal building model comprising three states

E. Test cases and data

The building model parameters, cf. Table I, can be obtained from the open-source building typology tool TABULA [37], providing information for a large number of different buildings in European countries. The disturbance profiles for occupancy and appliances are derived according to normed profiles for the according building class. Solar gains are computed for each building using weather data and building information

such as dimensioning of windows, orientation of the building, etc.

F. Model predictive control algorithm

Model Predictive Control (MPC) is a control strategy that uses a dynamic model of a system to optimize its performance over a specified time horizon in the future. The control algorithm solves the following optimization problem in each time step to find the optimal heat pump supply temperature for minimal heat pump power consumption while satisfying control bounds and state constraints. Heat pump power is computed from the heat pump thermal power produced and the COP as detailed in Section IV-D. To simulate sensor noise, as equally in the RL environment, we consider an initial value with additive random noise ϵ , randomly sampled from $\mathcal{N}(0, 0.5)$.

$$\begin{aligned} \min_{T_{\text{hp,sup}}} & \int_{t=0}^{t^N} P_{\text{el}}(t) dt \\ \text{s.t. } & T_{\text{room}}(0) = T_{\text{room,meas}} + \epsilon \\ & \text{system dynamics 9-10} \\ & T_{\text{room}}(t) \in \mathcal{Y} = [y_{\text{min}}, y_{\text{max}}] \quad \forall t \\ & T_{\text{hp,sup}}(t) \in \mathcal{U} = [u_{\text{min}}, u_{\text{max}}] \quad \forall t \end{aligned}$$

For more details about the implementation for MPC, we refer to [38].

V. EXPERIMENTS

A. Experiment Setup

a) Environment: To evaluate different constrained RL algorithms, we selected two buildings based on real-world examples. Building 1, an older structure equipped with a water heat pump and ground collectors, suffers from lower energy efficiency due to inadequate thermal insulation. In contrast, Building 2 is a newer construction utilizing an air-source heat pump. The simulations incorporate actual weather data relevant to the locations of these buildings and also consider internal gains from occupants. Additionally, we introduce additive noise $\mathcal{N}(0, 0.5)$ to the controller’s observations to assess performance under noisy conditions.

Our simulations employ a three-state building model with a simulation interval of 15 minutes per step. The observation space for the controllers includes ambient temperature, room temperature, wall temperature, return water temperature from the heat pump, and energy contributions from alternative heat sources (such as solar radiation and internal gains). The only action available to the controllers is adjusting the heat pump’s set temperature. We’ve established a reference set-point room temperature of 20 Celsius as a constraint. The key performance indicators (KPIs) are electrical energy consumption measured in kWh, and average and maximum comfort deviation, measured as the difference between actual and reference room temperatures, with deviations considered in both positive and negative directions. According to the application requirements, the average deviation must be below 0.05K, and the maximum deviation must be below 2.5K to be deemed acceptable.

To ensure a fair comparison across all algorithms, we standardized the hyperparameters and neural network architectures used. For more detailed information, please refer to Table II.

b) Training Setup: The heating system presents a unique challenge for constrained reinforcement learning (RL) algorithms, primarily due to the nature of its data distribution. In the real world, most transitions within such systems do not breach constraints, tending to cluster within a narrow band of the data spectrum. RL methods, which initially lack any specific guidance, must refine their strategies through a process of trial and error. To facilitate exploration across diverse data regimes, the training protocol sets episode lengths at 96 steps, corresponding to a day. After each episode, the environment resets to a randomly chosen initial state, aiding the RL agent in learning to navigate out of potentially unsafe states. To assess the performance of these RL algorithms, evaluations are conducted every 10 episodes, with each evaluation episode covering an entire year. We train our RL algorithms with 10000 episodes/days in the simulation.

For MPC, we leverage the simulator’s ground-truth dynamics model for prediction purposes. The temperature slack variable’s weighting factor is fixed at 0.1, aiming to balance between maintaining comfort and minimizing energy costs.

HYPERPARAMETERS	VALUE
BATCH SIZE	256
NETWORK ARCHITECTURE	[256,256]
DISCOUNT FACTOR γ	0.99
RANDOM STEPS	100
RL UPDATE FREQUENCY	1
BUFFER SIZE	3E6
COST LIMIT	10
LOG BARRIER FACTOR	10
LEARNING RATE	1E-3
POLYAK UPDATE FACTOR	0.005

TABLE II: The hyperparameters

c) Baselines Algorithms: We benchmark the following algorithms: (a) **SAC** [22] with reward shaping: we add a penalty reward of -2/-30 when the constraint is violated, which is tuned by [39]. (b) **SAC-Lagrangian** [21] (c) **CPO** [16] (d) **CSAC-LB** [34] (e) **MPC** [38].

B. Experiment Results and Analysis

Considering performance during training, he exemplarized for Building 1, as illustrated in Fig. 5, shows CSAC-LB’s superior exploration capabilities and robust training relative to other constrained RL algorithms. Unlike SAC-Lag, which demonstrates undesired training behavior distancing it from the optimal Pareto frontier (indicated by a varied color palette), CSAC-LB maintains a closer proximity to the threshold of minimal constraint violations for extended periods. This performance shows CSAC-LB’s efficacy, which can be explained by the advantages using log barrier methods, which guides the exploration into more critical regions effectively, which matches our statement of why we apply CSAC-LB to heating system mentioned in Sec III-D.

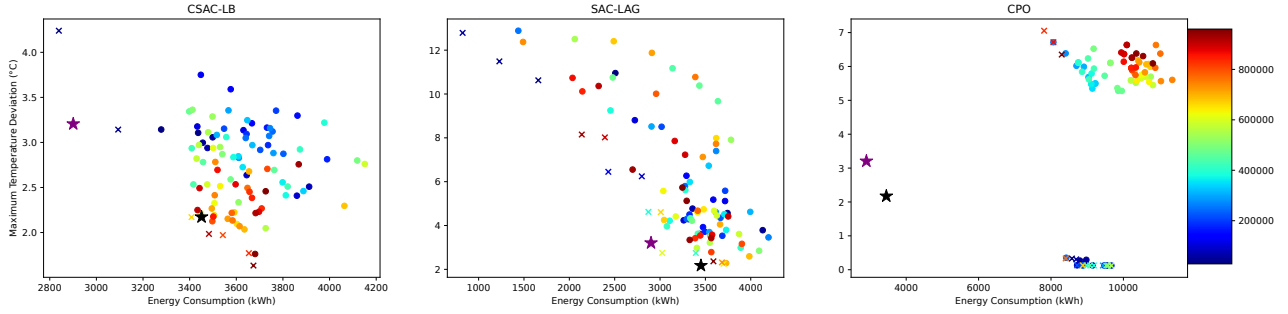


Fig. 5: Illustration of the constrained RL algorithms evaluation results during training in Building 1 without noise at seed 1. Each data point represents one evaluation episode and its color represents the number of training steps when the evaluation is performed. The y-axis is the maximum temperature deviation and the x-axis is the energy usage. Crosses mark evaluations on the Pareto front. Black/Purple star represents MPC and Rule-based Controller results respectively. CSAC-LB is able to explore more on the boundary during the training compared to SAC-LAG and CPO.

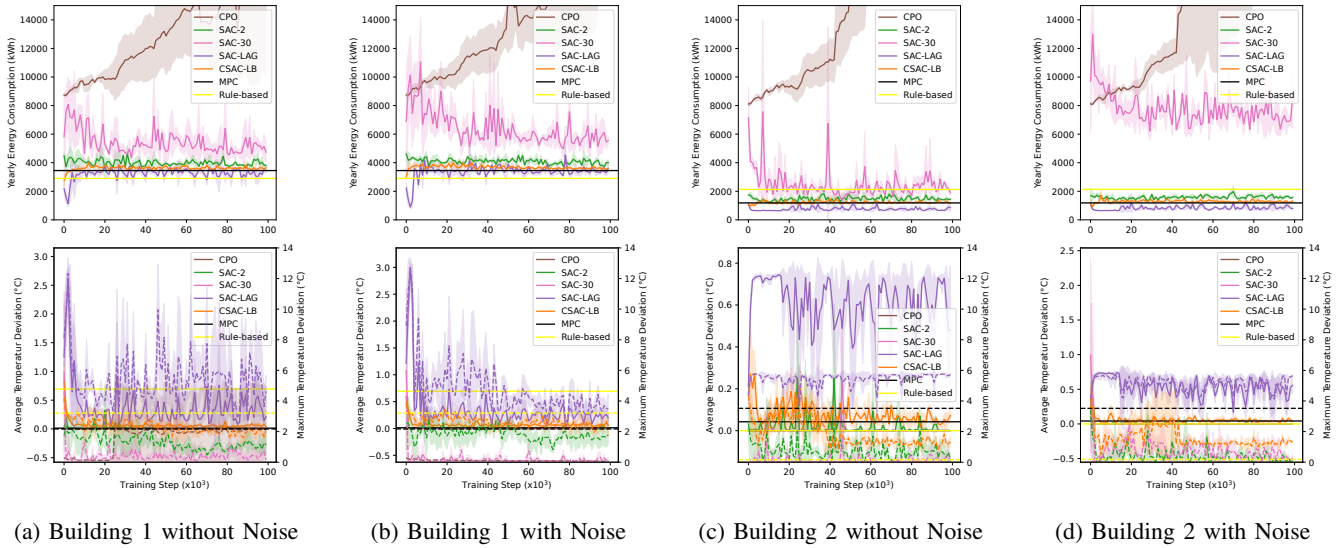


Fig. 6: The mean and std of the evaluation results of different constrained RL algorithms obtained by averaging over 3 seeds. x axis shows the number of training steps and y axis on the top row shows the total amount of electricity usage in a year. The bottom row shows the average temperature deviation in each step and the maximum temperature deviation (dashed line) throughout the year. MPC controller results are shown in black lines.

Figure 6 shows the performance of the different RL algorithms during training, as compared to MPC. Figure 6 reveals that CPO experiences training divergence; although it ensures satisfactory thermal comfort in most cases (except in Building 1 without noise), its energy usage escalates throughout training, signifying unstable training. SAC-Lag displays unstable training patterns across all test environments, failing to meet expectations in both thermal comfort and energy efficiency. Both SAC variants secure adequate thermal comfort but at the cost of increased energy consumption, accompanied by noisy training trajectories characterized by significant fluctuations. Contrary to expectations, the MPC method falls short of the performance achieved by other RL algorithms in Building 2 when compared to Building 1, hinting at a potential need for comprehensive hyperparameter tuning, whereas, the RL controllers use the same set of

hyperparameter, which demonstrates its robustness to different environments. Notably, all algorithms except MPC exhibit comparable performances when faced with noisy inputs across different buildings, showing its sensitivity to input noise. CSAC-LB stands out by effectively navigating the balance between thermal comfort and energy usage, minimizing temperature deviations and energy consumption without major constraint violation.

To summarize, performance is always a trade-off between comfort (or safety) and energy efficiency. In practical applications, controlling comfort deviation, which in this context equates to safety, is crucial. Based on the yearly energy consumption and comfort deviation metrics presented in Table III, only MPC and CSAC-LB, followed by SAC-2, show good performance in terms of energy efficiency while maintaining low comfort deviation. CPO results in significantly higher energy consumption, whereas SAC-Lag

exhibits unacceptable comfort deviations. MPC performs well in the absence of noise but falls short when model-plant mismatches, in the form of noise, are present.

VI. CONCLUSION

In this study, we apply the recently developed constrained RL algorithm CSAC-LB to the critical problem of energy-efficient heat pump temperature control. The goal is to operate the heat pump with low electricity consumption while reliably maintaining indoor temperature bounds during both training and operation. To achieve this, we introduce I4B, a lightweight, open-source simulation framework specifically designed for building heat pump control. I4B provides extensive customization options and simulates various real-world building scenarios, thereby bridging the gap between the control and RL communities with its user-friendly interfaces.

Our evaluation of constrained RL algorithms reveals CSAC-LB's suitability for heat pump control. By leveraging a linear smoothed log barrier function and a double-Q network, CSAC-LB effectively addresses common underestimation issues and promotes boundary exploration—key for heating control tasks. Among the five recent RL algorithms tested, CSAC-LB stands out for its resilience to noisy data, adeptly balancing thermal comfort and energy efficiency. Considering model-plant mismatch in the form of noise, CSAC-LB demonstrates its superiority over MPC.

Future directions include integrating weather forecasts and model-based methods into the constrained RL approach and expanding I4B to encompass multi-room building setups.

Algo	Building1 wo noise			Building1 w noise			Building2 wo noise			Building2 with noise		
	Energy	Avg. D	Max. D	Energy	Avg. D	Max. D	Energy	Avg. D	Max. D	Energy	Avg. D	Max. D
CPO	19724	0.0055	2.076	24269	0.0000	0.063	30900	0.0000	0.000	27564	0.0000	0.000
SAC-2	3803	0.0034	1.126	4017	0.0035	1.782	1433	0.0001	0.150	1569	0.0000	0.072
SAC-30	4729	0.0000	0.160	5542	0.0001	0.153	1897	0.0000	0.064	2588	0.0000	0.000
SAC-Lag	3452	0.2119	4.637	3584	0.1991	3.468	852	0.4815	5.704	797	0.5593	5.664
CSAC-LB	3652	0.0471	2.010	3608	0.0603	2.373	1178	0.0727	1.328	1312	0.0445	1.309
MPC	3451	0.0135	2.173	4450	0.0103	1.969	1186	0.0424	3.518	1819	0.0307	3.243

TABLE III: Summary of KPIs regarding electrical energy consumption (in kWh) and average and maximum deviation (in K) for two different buildings with and without noise. Acceptable KPI values concerning comfort deviation are marked in bold. Concerning energy consumption, the values in the lowest 50% are marked in bold.

REFERENCES

- [1] T. Haarnoja, S. Ha, A. Zhou, J. Tan, G. Tucker, and S. Levine, "Learning to walk via deep reinforcement learning," in *Robotics: Science and Systems XV, Freiburg, Germany, June 22-26, 2019*, A. Bicchi, H. Kress-Gazit, and S. Hutchinson, Eds., 2019.
- [2] V. Makoviychuk, L. Wawrzyniak, Y. Guo, M. Lu, K. Storey, M. Macklin, D. Hoeller, N. Rudin, A. Allshire, A. Handa, and G. State, "Isaac gym: High performance GPU based physics simulation for robot learning," in *NeurIPS Datasets and Benchmarks 2021, December 2021, virtual*, 2021.
- [3] Z. Fu, A. Kumar, J. Malik, and D. Pathak, "Minimizing energy consumption leads to the emergence of gaits in legged robots," in *Conference on Robot Learning, 8-11 November 2021, London, UK*, ser. Proceedings of Machine Learning Research, vol. 164. PMLR, 2021, pp. 928–937.
- [4] Z. Nagy, G. Henze, S. Dey, J. Arroyo, L. Helsen, X. Zhang, B. Chen, K. Amasyali, K. Kurte, A. Zamzam, et al., "Ten questions concerning reinforcement learning for building energy management," *Building and Environment*, vol. 241, p. 110435, 2023.
- [5] S. Brandi, M. S. Piscitelli, M. Martellacci, and A. Capozzoli, "Deep reinforcement learning to optimise indoor temperature control and heating energy consumption in buildings," *Energy and Buildings*, vol. 224, p. 110225, 2020.
- [6] A. Nagy, H. Kazmi, F. Cheaib, and J. Driesen, "Deep reinforcement learning for optimal control of space heating," *arXiv preprint arXiv:1805.03777*, 2018.
- [7] T. Rohrer, L. Frison, L. Kaupenjohann, K. Scharf, and E. Hergenrother, "Deep reinforcement learning for heat pump control," in *Lecture Notes in Networks and Systems*, ser. LNNS, vol. 711. Springer, 2023.
- [8] "Reinforced model predictive control (rl-mpc) for building energy management," *Applied Energy*, vol. 309, p. 118346, 2022.
- [9] L. Frison and S. Gözlhäuser, "Adaptive neural network based control approach for building energy control under changing environmental conditions," in *Proceedings of the 6th Annual Learning for Dynamics & Control Conference*, ser. Proceedings of Machine Learning Research, vol. 242. PMLR, 15–17 Jul 2024, pp. 1741–1752. [Online]. Available: <https://proceedings.mlr.press/v242/frison24a.html>
- [10] J. García and F. Fernández, "A comprehensive survey on safe reinforcement learning," *J. Mach. Learn. Res.*, vol. 16, pp. 1437–1480, 2015.
- [11] G. Dulac-Arnold, N. Levine, D. J. Mankowitz, J. Li, C. Paduraru, S. Gowal, and T. Hester, "Challenges of real-world reinforcement learning: definitions, benchmarks and analysis," *Mach. Learn.*, vol. 110, no. 9, pp. 2419–2468, 2021.
- [12] E. Uchibe and K. Doya, "Constrained reinforcement learning from intrinsic and extrinsic rewards," in *2007 IEEE 6th International Conference on Development and Learning*, 2007, pp. 163–168.
- [13] H. Bou-Ammar, R. Tutunov, and E. Eaton, "Safe policy search for lifelong reinforcement learning with sublinear regret," in *Proceedings of the 32nd International Conference on Machine Learning, ICML 2015, Lille, France, 6-11 July 2015*, ser. JMLR Workshop and Conference Proceedings, vol. 37. JMLR.org, 2015, pp. 2361–2369.
- [14] L. Yang, J. Ji, J. Dai, L. Zhang, B. Zhou, P. Li, Y. Yang, and G. Pan, "Constrained update projection approach to safe policy optimization," in *Annual Conference on Neural Information Processing Systems 2022, NeurIPS 2022, New Orleans, LA, USA, November 28 - December 9, 2022*, 2022.
- [15] K. Polymenakos, A. Abate, and S. Roberts, "Safe policy search using gaussian process models," in *Proceedings of the 18th international conference on autonomous agents and multiagent systems*, 2019, pp. 1565–1573.
- [16] J. Achiam, D. Held, A. Tamar, and P. Abbeel, "Constrained policy optimization," in *Proceedings of the 34th International Conference on Machine Learning, ICML 2017, Sydney, NSW, Australia, 6-11 August 2017*, ser. Proceedings of Machine Learning Research, D. Precup and Y. W. Teh, Eds., vol. 70. PMLR, 2017, pp. 22–31.
- [17] Y. Zhang, Q. Vuong, and K. W. Ross, "First order constrained optimization in policy space," in *Annual Conference on Neural Information Processing Systems 2020, NeurIPS 2020, H. Larochelle, M. Ranzato, R. Hadsell, M. Balcan, and H. Lin, Eds.*, 2020.
- [18] Y. Chow, A. Tamar, S. Mannor, and M. Pavone, "Risk-sensitive and robust decision-making: a cvar optimization approach," in *Annual Conference on Neural Information Processing Systems 2015, December 7-12, 2015, Montreal, Quebec, Canada*, C. Cortes, N. D. Lawrence, D. D. Lee, M. Sugiyama, and R. Garnett, Eds., 2015, pp. 1522–1530.
- [19] Y. Chow, M. Ghavamzadeh, L. Janson, and M. Pavone, "Risk-constrained reinforcement learning with percentile risk criteria," *J. Mach. Learn. Res.*, vol. 18, pp. 167:1–167:51, 2017.
- [20] S. Ha, P. Xu, Z. Tan, S. Levine, and J. Tan, "Learning to walk in the real world with minimal human effort," in *4th Conference on Robot Learning, CoRL 2020, 16-18 November 2020, Virtual Event / Cambridge, MA, USA*, ser. Proceedings of Machine Learning Research, vol. 155. PMLR, 2020, pp. 1110–1120.
- [21] J. Achiam, "Exploration and safety in deep reinforcement learning," Ph.D. dissertation, EECS Department, University of California, Berkeley, May 2021.
- [22] T. Haarnoja, A. Zhou, P. Abbeel, and S. Levine, "Soft actor-critic: Off-policy maximum entropy deep reinforcement learning with a stochastic actor," in *Proceedings of the 35th International Conference on Machine Learning, ICML 2018, Stockholm, Sweden, July 10-15, 2018*, ser. Proceedings of Machine Learning Research, J. G. Dy and A. Krause, Eds., vol. 80. PMLR, 2018, pp. 1856–1865.
- [23] Q. Yang, T. D. Simão, S. H. Tindemans, and M. T. J. Spaan, "WC-SAC: worst-case soft actor critic for safety-constrained reinforcement learning," in *Thirty-Fifth AAAI Conference on Artificial Intelligence, AAAI 2021, Virtual Event, February 2-9, 2021*. AAAI Press, 2021, pp. 10 639–10 646.
- [24] C. Zeng and H. Zhang, "A logarithmic barrier method for proximal policy optimization," *CoRR*, vol. abs/1812.06502, 2018.
- [25] Y. Liu, J. Ding, and X. Liu, "IPO: interior-point policy optimization under constraints," in *The Thirty-Fourth AAAI Conference on Artificial Intelligence, AAAI 2020, New York, NY, USA, February 7-12, 2020*. AAAI Press, 2020, pp. 4940–4947.
- [26] F. Berkenkamp, M. Turchetta, A. P. Schoellig, and A. Krause, "Safe model-based reinforcement learning with stability guarantees," in *Annual Conference on Neural Information Processing Systems 2017, December 4-9, 2017, Long Beach, CA, USA*, 2017, pp. 908–918.
- [27] P. Scharnhorst, B. Schubnel, C. Fernández Bandera, J. Salom, P. Taddeo, M. Boegli, T. Gorecki, Y. Stauffer, A. Peppas, and C. Politi, "Ergym: A building model library for controller benchmarking," *Applied Sciences*, vol. 11, no. 8, 2021.
- [28] D. Blum, J. Arroyo, S. Huang, J. Drgoña, F. Jorissen, H. T. Walnum, Y. Chen, K. Benne, D. Vrabie, M. Wetter, and L. Helsen, "Building optimization testing framework (bopstest) for simulation-based benchmarking of control strategies in buildings," *Journal of Building Performance Simulation*, vol. 14, no. 5, pp. 586–610, 2021.
- [29] J. Jiménez-Raboso, A. Campoy-Nieves, A. Manjavacas-Lucas, J. Gómez-Romero, and M. Molina-Solana, "Sinergym: a building simulation and control framework for training reinforcement learning agents." New York, NY, USA: Association for Computing Machinery, 2021.
- [30] M. Towers, J. K. Terry, A. Kwiatkowski, J. U. Balis, G. d. Cola, T. Deleu, M. Goulão, A. Kallinteris, A. KG, M. Krimmel, R. Perez-Vicente, A. Pierré, S. Schulhoff, J. J. Tai, A. T. J. Shen, and O. G. Younis, "Gymnasium," Mar. 2023.
- [31] A. Findeis, F. Kazhamiaka, S. Jeen, and S. Keshav, "Beobench: a toolkit for unified access to building simulations for reinforcement learning." New York, NY, USA: Association for Computing Machinery, 2022.
- [32] H. Kervadec, J. Dolz, J. Yuan, C. Desrosiers, E. Granger, and I. B. Ayed, "Constrained deep networks: Lagrangian optimization via log-barrier extensions," 2019.
- [33] S. Boyd and L. Vandenberghe, *Convex Optimization*. Cambridge University Press, 2004.
- [34] B. Zhang, Y. Zhang, L. Frison, T. Brox, and J. Bödecker, "Constrained reinforcement learning with smoothed log barrier function," 2024.
- [35] J. Ji, B. Zhang, J. Zhou, X. Pan, W. Huang, R. Sun, Y. Geng, Y. Zhong, J. Dai, and Y. Yang, "Safety gymnasium: A unified safe reinforcement learning benchmark," in *Annual Conference on Neural Information Processing Systems 2023, NeurIPS 2023, New Orleans, LA, USA, December 10 - 16, 2023*, 2023.
- [36] G. Brockman, V. Cheung, L. Pettersson, J. Schneider, J. Schulman, J. Tang, and W. Zaremba, "Openai gym," 2016.
- [37] "TABULA WebTool," <https://webtool.building-typology.eu>, 2017 (accessed August 10, 2022).
- [38] L. Frison, M. Kleinstück, and P. Engelmann, "Model-predictive control for testing energy flexible heat pump operation within a hardware-in-the-loop setting," *Journal of Physics: Conference Series*, vol. 1343, no. 1, p. 012068, nov 2019.
- [39] Y. Luo and T. Ma, "Learning barrier certificates: Towards safe reinforcement learning with zero training-time violations," in *Annual*

Conference on Neural Information Processing Systems 2021, NeurIPS 2021, December 6-14, 2021, virtual, M. Ranzato, A. Beygelzimer, Y. N. Dauphin, P. Liang, and J. W. Vaughan, Eds., 2021, pp. 25 621–25 632.